Influence of amplitude-phase coupling on the dynamics of semiconductor lasers subject to optical feedback

T. Heil, I. Fischer, and W. Elsäßer
Institute of Applied Physics, Darmstadt University of Technology, Schloßgartenstrasse 7, D-64289 Darmstadt, Germany
(Received 16 February 1999)

We present extensive experimental investigations of the dynamics of semiconductor lasers subject to optical feedback in dependence on the linewidth enhancement factor α which accounts for the amplitude phase coupling of the optical field. A reduction of α leads to conspicuous changes of the dynamics of the system which are characterized and classified in the phase space of feedback strength versus injection current, thus demonstrating the importance of α as the system's main nonlinearity. In particular, we demonstrate a drastic extension of the regime of coexistence between coherence collapsed dynamics and stable emission, and an increased stability of this stable emission state. We show that a theoretical analysis of the Lang-Kobayashi rate equation model provides a qualitative understanding of the physical mechanisms underlying the observed dynamical behavior and its dependence on α. Finally, being able to control the nonlinearity of the system, we open up new perspectives for the stabilization of semiconductor lasers subject to moderate to strong optical feedback. [S1050-2947(99)06307-6]

PACS number(s): 42.65.Sf, 42.55.Px

I. INTRODUCTION AND OVERVIEW

Semiconductor lasers subject to optical feedback from external reflectors like the front facet of an optical fiber, a mirror, or a compact disk exhibit a rich variety of dynamical phenomena which can degrade their performance in possible applications. Thus, a profound understanding of these dynamical phenomena is indispensable in order to avoid the instabilities or to stabilize and control the semiconductor laser emission. Besides their great practical importance, semiconductor lasers subject to optical feedback from an external cavity are an attractive model system for the study of the universal aspects of delay-induced instabilities: several different routes to chaos including the quasiperiodic route [1], the period doubling route [2], the Ikeda scenario [3,4], and crisis [5], have already been identified in semiconductor laser with optical feedback, which again contributed to the understanding of delay systems in general.

The complex dynamical behavior of semiconductor lasers subject to delayed optical feedback is linked to the following two important aspects: first, the infinite number of possible degrees of freedom available for the system due to the time-delayed feedback, and second, the nonlinear amplitude-phase coupling of the electrical field which is particularly strong for semiconductor lasers. This nonlinear amplitude-phase coupling is caused by the carrier-induced variation of real and imaginary parts of the semiconductor material's susceptibility $\chi(n)=\chi_r(n)+i\chi_i(n)$, and is described by the linewidth enhancement factor α [6,7],

$$\alpha=-\frac{d[\chi_r(n)]/dn}{d[\chi_i(n)]/dn}. \tag{1}$$

As one of the fundamental parameters for semiconductor lasers, α causes the enhancement of the laser linewidth [7] and is of decisive importance for many dynamical processes such as modulation response, frequency chirp, and, in particular, optical feedback effects [8]. Up to now, both α and the emission wavelength have always been considered as fixed parameters of the investigated semiconductor laser. Indeed, tuning the emission wavelength of the laser by shifting the gain profile of the solitary laser, e.g., by temperature tuning, affects the value of α only very slightly. However, by tuning the emission wavelength of the laser away from its solitary gain maximum without changing the gain profile of the solitary laser, substantial changes of the value of α can be achieved [9]: experiments showed that even a transition to negative values of α occurs for wavelengths much shorter than the solitary gain maximum wavelength [10]. Theoretical studies have already drawn attention to the influence of the linewidth enhancement factor α on the dynamical behavior of semiconductor lasers with optical feedback [11,12]; however, experimental investigations of this important point are still lacking.

In this paper, we concentrate on the dynamics of semiconductor lasers subject to optical feedback in dependence on the three most relevant parameters, the injection current I, the optical feedback strength γ, and, in particular, the linewidth enhancement factor α. We control α by tuning the emission wavelength of the laser away from its solitary gain maximum by using an intracavity etalon. For each of several different values of α, we record γ-I-space diagrams which map the dynamical behavior of the system by identifying distinct dynamical regimes. Using this method, we provide detailed information about the effect of the variation of α on the dynamics of the system over wide ranges of relevant parameters. In particular, we give experimental evidence that the stability of the system increases with decreasing wavelengths, i.e., decreasing α. We find that the parameter regimes of the recently reported coexistence of low-frequency fluctuations (LFF) and stable emission on a single external-cavity mode [13] enlarge drastically for decreasing α. For the lowest value of α, possible stable emission expands even into the regime of the fully developed coherence collapse. Furthermore, we investigate the effect of changing α on the relevant physical mechanisms underlying the coherence collapse dynamics. Our results demonstrate that semiconductor lasers subject to optical feedback are delay systems with a

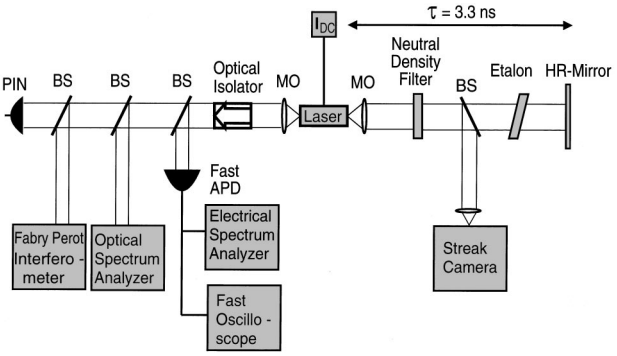

FIG. 1. Experimental setup.

controllable nonlinearity, and, thus, become even more interesting as a model system for further experimental studies of delay phenomena in general.

The paper is structured as follows. Section II describes the experimental setup and the implementation of the experiments. In Sec. III, we present our experimental results and identify the effects of a variation of α on the dynamical behavior of semiconductor lasers subject to optical feedback. Section IV reviews some theoretical results obtained from an analysis of the Lang-Kobayshi rate equation model [14] which are relevant for the discussion, and the understanding of our experimental results. Section V, finally, provides a short summary and presents our conclusions.

II. SETUP AND EXPERIMENTAL IMPLEMENTATION

In the experiments, we use a bulk Fabry-Pérot laser diode (Hitachi HLP1400), which is best known with respect to experiments on delay-induced instabilities. Figure 1 shows a scheme of the experimental setup. The laser diode is driven by an ultralow noise dc-current source, its temperature stabilized to better than 0.01K. The laser beam is collimated by an anti-reflection-coated microscope objective (MO). The feedback branch consists of a high reflection mirror of interferometric flatness better than $\lambda/200$, and a neutral density filter to vary the optial feedback strength. The delay time of the external cavity amounts to 3.3 ns, which corresponds to an external cavity mode spacing of 300 MHz. A key element of the setup is the intracavity etalon with a transmission bandwidth of 5 nm, corresponding to approximately 2.1 THz. This spectral selectivity of the etalon is selected to cause single mode operation of the semiconductor laser in the LFF regime. However, it does not suppress the corresponding external cavity modes due to its large transmission bandwidth. The etalon allows us to tune the emission wavelength of the laser over a range of about 10 nm around the solitary gain maximum maintaining single mode operation. In order to account for the wide temporal and optical scales which play an important role in the dynamics of external cavity semiconductor lasers, both the intensity time series and the optical spectrum are measured simultaneously on several different resolution stages. The intensity dynamics is detected by a single shot streak camera with an analog bandwidth of more than 50 GHz and by a fast avalanche photodiode (APD) of larger than 3 GHz bandwidth. The power spectrum of the APD signal is recorded by an electrical spectrum analyzer of 0.1 kHz to 21 GHz bandwidth. The corresponding time series are low-pass filtered with the cutoff frequency at 1 GHz and detected by a fast single shot digital oscilloscope of the same bandwidth. The time-averaged intensity is measured by a *p-i-n* photodiode. The optical spectrum is analyzed via a grating spectrometer with a resolution of 0.1 nm in order to resolve the longitudinal diode modes and to monitor the absolute emission wavelength of the laser. In addition, a confocal scanning Fabry-Pérot interferometer is used to resolve the external cavity modes. The free spectral range of the interferometer amounts to 2 GHz, the resolution to 10 MHz. An optical isolator shields the laser from unwanted external feedback from the detection branch.

The experiments are performed as follows. Using the above setup, we exploit the strong spectral dependence of α [10,15]: by tilting the intracavity etalon, we tune the emission wavelength of the laser away from its solitary gain maximum, which remains unchanged. This allows us to tailor the value of α in a well controlled way. Having selected the desired value of α, we adjust the optical feedback strength γ by using the variable neutral density filter. The value of γ is determined by measuring the effective power reflectivity of the feedback branch [14]. Then, the injection current I is increased starting below threshold up to its maximum possible value. We investigate the resulting dynamical behavior of the system in dependence on I, and classify the dynamical behavior in distinct dynamical regimes. Finally, still keeping α constant, we repeat this procedure for several different values of γ. Thus, for the selected value of α, we obtain a map displaying the dynamical behavior of the system classified in several distinct dynamical regimes in γ-I space. Using the method described above, we record several γ-I-space maps for different values of α. Comparing these phase-space maps, we provide both detailed information and a global survey about the impact of changing α on the dynamics of semiconductor lasers subject to delayed optical feedback.

III. EXPERIMENTAL RESULTS

In this section, we first discuss the measurement of the spectral dependence of α. Then, we present three representative γ-I-space diagrams recorded for three different values of α. The diagrams map the dynamical behavior of the system by identifying different dynamical regimes, which then are illustrated and characterized. Finally, the three diagrams are compared and discussed with respect to the reduction of α.

A. Spectral dependence of α

We have measured α according to the method proposed by Henning and Collins [16]. This method is based on net gain measurements obtained from the modulation depths introduced by Fabry-Pérot resonances into the spontaneous emission spectrum of the laser [17]. The accuracy of the obtained values of α is limited by the precision of the wavelength shift and the modulation depth measurements.

Figure 2 depicts the plot of the spectral dependence of α of the HLP1400 laser diode including error bars. Obviously, α decreases continuously with decreasing wavelength. The spectral dependence of α and the absolute values for α shown in Fig. 2 are in good agreement, both with calculated

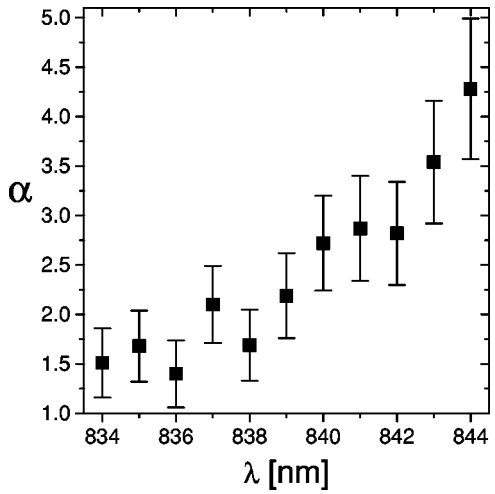

FIG. 2. Spectral dependence of the linewidth enhancement factor α for a HLP1400 laser diode. The gain maximum of the solitary laser is at 840 nm.

α spectra [15] and with previously obtained experimental results for this type of laser diode [18].

In a linear approximation around the solitary laser threshold, α is given by

$$\alpha = -2k\frac{d\mu/dn'}{dg/dn'}, \tag{2}$$

where $d\mu$ and dg are the changes of refractive index and gain per length, respectively, which occur when the carrier density n' is varied [18]; k is the free-space wave vector. Time-resolved gain spectroscopy experiments have shown that the spectral dependence of the relative change of the refractive index $d\mu$ is distinctly smaller than the change of the gain per length dg [10]. Thus, the wavelength dependence of α depicted in Fig. 2 is dominated by the strong increase of the differential gain $\xi \propto dg$ with decreasing wavelength.

Having determined the relation between the quantitative values of α and the emission wavelengths within the accessible tuning range, we are now able to investigate the effect of a reduction of α on the dynamical behavior of the system.

B. Characterization of the occurring dynamical regimes

Figure 3 depicts three γ-I-space diagrams for three different emission wavelengths, i.e., three different values of α: Fig. 3(a), $\lambda = 841$ nm corresponding to $\alpha = 2.8 \pm 0.5$; Fig. 3(b), $\lambda = 838.2$ nm corresponding to $\alpha = 2.1 \pm 0.4$; and Fig. 3(c), $\lambda = 835.5$ nm corresponding to $\alpha = 1.6 \pm 0.3$. Figure 3 shows that the system exhibits similar dynamical regimes for each of the three different α factors. However, the extension of these regimes varies significantly depending on α. The dynamical behavior corresponding to the regimes is illustrated by Fig. 4, which depicts typical intensity time series recorded for the respective parameters. Very close to the feedback-reduced lasing threshold, the laser emits apparently stably on several external cavity modes. Increasing the injection current slightly, the LFF regime is reached. Figure 4 (top) shows a typical LFF time series characterized by sudden intensity dropouts on a microsecond-to-nanosecond time

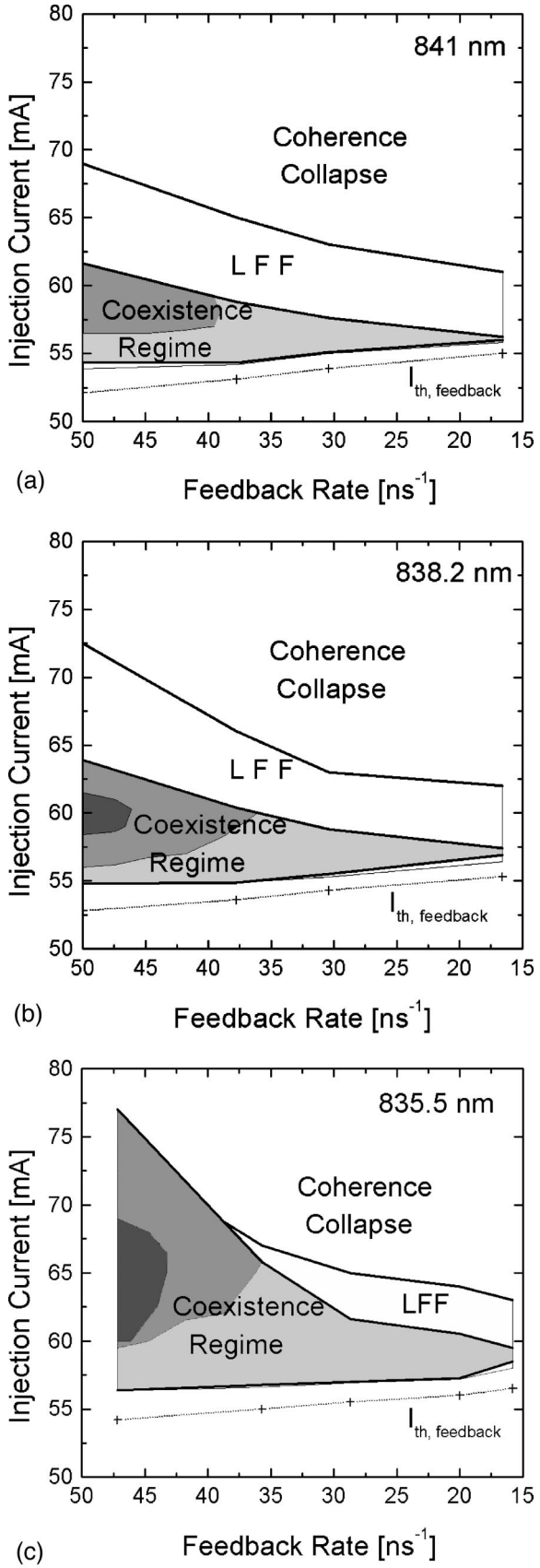

FIG. 3. The dynamical behavior of semiconductor lasers subject to delayed optical feedback in dependence on the injection current I and the optical feedback strength γ for (a) 841 nm corresponding to $\alpha = 2.8(\pm 0.5)$, (b) 838.2 nm corresponding to $\alpha = 2.1(\pm 0.4)$, and (c) 835.5 nm corresponding to $\alpha = 1.6(\pm 0.3)$.

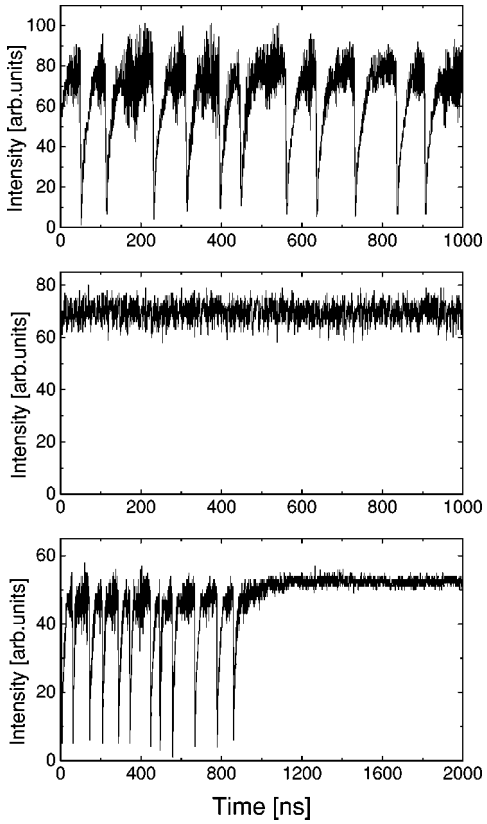

FIG. 4. Single-shot intensity time series low pass filtered with a cutoff frequency at 1 GHz. Top: low-frequency fluctuations recorded for $I=58$ mA and $\gamma=25$ ns^{-1}. Middle: fully developed coherence collapse recorded for $I=70$ mA and $\gamma=25$ ns^{-1}. Bottom: coexistence of low-frequency fluctuations and stable emission on a single high-gain external-cavity mode recorded for $I=60$ mA and $\gamma=50$ ns^{-1}. All time series are recorded for $\lambda=839.7$ nm.

scale, a behavior which has been vividly discussed during recent years [19–21]. Increasing the injection current further, the time intervals between subsequent intensity dropouts shorten; finally, the dropouts begin to merge and a continuous transition to the fully developed coherence collapse (CC) takes place. The CC is characterized by a very broad power spectrum and completely irregular intensity time series, as depicted by Fig. 4 (middle).

A striking phenomenon occurring over a large parameter region is the recently discovered coexistence of LFF with a stable high-power state, in which the laser emits on a single external cavity mode [13]. Figure 4 (bottom) depicts a typical time series recorded within the coexistence regime. In this time series, a transition from LFF to stable emission occurs at the time of 1000 ns. The duration of the stable emission state in comparison with the duration of the LFF state strongly depends on the injection current and the feedback strength, i.e., the position in γ-I space. In order to account for this parameter dependence, we encode the coexistence regime, as depicted in Fig. 3, by three different shades of gray: dark gray represents the parameter region in which the duration of the stable emission states is longest; time intervals of stable emission typically exceed 1 min, only interrupted by short time intervals of LFF emission; intermediate gray represents the region in which the system jumps back and forth between LFF and stable emission, typically on a time scale of seconds; light gray represents the region in which the LFF prevail, and the stable state is only reached for short times, typically milliseconds.

The dynamical behavior of the system classified in parameter space by the distinct dynamical regimes described above is strongly dependent on the value of α. In the following, we compare the three γ-I-space diagrams in order to identify the effects of this α dependence.

C. α dependence of the dynamical behavior

In this subsection, we summarize the key results obtained from a comparison of the three γ-I-space diagrams depicted in Fig. 3. We find that the following phenomena are associated with a reduction of the α.

(i) Enlargement of the coexistence regime. The regions of coexistence of the LFF state and the state of stable emission on a single external-cavity mode enlarge drastically for decreasing α.

(ii) Increased stability of the stable state. The parameter regime of very long times of stable emission, depicted in dark gray in the γ-I-space diagrams, expands substantially for decreasing α.

(iii) Coexistence of CC and stable emission. For the lowest investigated value of $\alpha=1.6\pm0.3$, the coexistence region exceeds the LFF regime. Thus, for stronger feedback and higher injection currents, we observe a coexistence of the stable emission state with the fully developed CC. Moreover, the signature of the stable state remains the same while the continuous transition from LFF to the fully developed CC occurs.

(iv) Properties of the LFF regime. Within the investigated range of parameters, the extension of the LFF regime does not change as significantly as the coexistence regime with decreasing α. Also, the temporal signature of the LFF and the mean time interval between subsequent intensity dropouts do not exhibit drastic changes.

IV. DISCUSSION

In order to discuss the experimental results listed above, we briefly review in this section some theoretical results obtained from an analysis of the standard rate equation model for semiconductor lasers subject to delayed optical feedback. We show that these theoretical results provide a qualitative understanding of our experimental findings.

A. Theoretical results

The basis of the theoretical model is the well-known Lang-Kobayashi rate equations [14] for the number of carriers $n(t)=N(t)-N_0$ with respect to the solitary threshold level N_0, and the slowly varying complex electrical field amplitude $E(t)$:

$$\dot{E}(t)=\frac{1}{2}(1+i\alpha)\xi n(t)E(t)+\gamma E(t-\tau)e^{-i\omega_0\tau}, \qquad (3)$$

$$\dot{n}(t)=(p-1)\frac{I_{\mathrm{th}}}{e}-\frac{n(t)}{T_1}-[\Gamma_0+\xi n(t)]P(t). \qquad (4)$$

In these equations, the optical feedback is taken into account by the feedback rate γ and the delay time τ. The elec-

trical field is normalized so that $P(t)=|E(t)|^2$ is the photon number; ω_0 represents the optical frequency of the solitary laser, ξ the differential gain, Γ_0 the cavity decay rate, T_1 the carrier lifetime, I_{th} the bias current at solitary laser threshold, e the electron charge, and p is the pump parameter. The analysis of the Lang-Kobayashi equations shows that the fixed points of the system consisting of the semiconductor laser cavity and the external cavity always occur in pairs of stable and unstable fixed points. The stable fixed points correspond to constructive interference of the coupled cavities and are usually referred to as *modes*. The unstable fixed points, which exhibit a saddle node instability, correspond to destructive interference of the coupled cavities and, thus, are called *antimodes*. Each fixed point of the system is defined by a constant optical frequency $(\omega_0+\Delta\omega)$ and a constant carrier number n given by the following equations [22]:

$$\Delta\omega\tau=\gamma\tau\sqrt{1+\alpha^2}\,\sin\{(\omega_0+\Delta\omega)\tau+\arctan\alpha\}, \tag{5}$$

$$(\gamma\tau)^2=\left(\Delta\omega\tau-\alpha\frac{\tau\xi n}{2}\right)^2+\left(\frac{\tau\xi n}{2}\right)^2. \tag{6}$$

According to Eqs. (5) and (6), modes and antimodes lie on an ellipse around the solitary laser mode in the $(\Delta\omega,n)$ space [23], which is physically caused by the strong amplitude-phase coupling in the semiconductor laser described by the nonvanishing α.

A linear stability analysis of the fixed points of the system shows that the previously stable modes destabilize for increasing optical feedback via Hopf bifurcations. However, at least one mode, the so-called maximum gain mode, on the very low-frequency high-gain side of the ellipse, always remains stable [24]. Furthermore, all modes in the vicinity of the maximum gain mode which satisfy

$$-\arctan(1/\alpha)<(\omega_0+\Delta\omega)\tau<0 \tag{7}$$

also remain stable [24]. Thus, according to Eq. (7), the number of stable high-gain modes (HGM) increases for decreasing α.

This structure of the fixed-point solutions of the Lang-Kobayashi equations in frequency-inversion space, and their stability properties, lead to the following interpretation of the dynamical phenomena observed for constant α.

1. LFF and coexistence

The LFF can be understood as an itinerancy of the trajectory of the system among the attractor ruins of the destabilized modes towards the stable HGM [22]. Consequently, the emitted power, which is organized in picosecond pulses [5], increases during this itinerancy. Due to the elliptic shape of the position of the fixed points, the basin boundaries of the attractor ruins of stable and unstable fixed points approach as the trajectory itinerates towards high gain. So, even a collision of these attractor ruins can occur, a process which is referred to as crisis. The characteristic power dropouts of the LFF are, thus, associated with such a crisis bouncing the trajectory away from its drift towards the stable HGMs. Then, the trajectory is reinjected into the lower gain part of the ellipse and the process restarts.

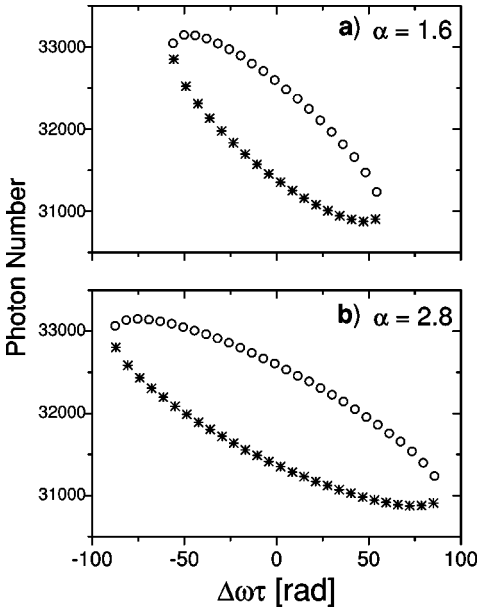

FIG. 5. Fixed points of the Lang-Kobayashi equations calculated for $\gamma=10\ \mathrm{ns}^{-1}$ and $\tau=3$ ns. (a) $\alpha=2.8$, (b) $\alpha=1.6$.

However, within the parameter ranges corresponding to the coexistence regime shown in Fig. 3, a crisis does not have to occur necessarily. Within these coexistence regimes, the trajectory has a finite probability to reach one of the stable HGMs before a crisis can take place [13]. The trajectory can stay on one of the stable HGMs for very long times until external perturbations or, right above threshold, spontaneous-emission noise, eject the trajectory away from the stable HGMs. Then the LFF restart, and a varying number of dropouts occurs until one of the stable HGMs is reached again.

In the following, we review theoretical results which describe the impact of a variation of α on the dynamical behavior described above.

2. Influence of α

The effect of a reduction of α on the structure of the solutions of the Lang-Kobayashi equations is illustrated by Fig. 5; it depicts two sets of fixed points calculated from Eqs. (5) and (6) for different values of α under otherwise identical conditions. In both cases, the fixed points are located on an ellipse in frequency-inversion space. However, the eccentricity of the ellipse reduces with decreasing α: for $\alpha=0$, the fixed points are located on a circle around the solitary diode mode. Consequently, the distance between modes and antimodes in frequency-inversion space increases for decreasing α. Furthermore, the total number of fixed points decreases, however according to Eq. (7), the number of the *stable* fixed points (the HGMs) increases. Thus, the trajectory does not have to itinerate along the whole ellipse in order to reach one of the stable HGM. Finally, as demonstrated by numerical simulations [12], the size of the local attractor of each single destabilized mode decreases for smaller values of α.

To sum up, the increased distance between the attractor ruins of stable and unstable fixed points, the reduced size of

the local attractors, and the shortened itinerancy towards high gain reduce substantially the probability for the occurrence of a crisis, but increase the probability that the trajectory reaches one of the stable HGMs.

B. Comparision between experimental and theoretical results

The effects of a reduction of α on the structure of the solutions of the Lang-Kobayashi equations reviewed in the preceding subsection provide the following physical interpretation of our experimental findings.

1. Enlargement of the coexistence regime

The most striking feature of the presented experimental results is the drastic enlargement of the regions of coexistence of LFF and stable emission with decreasing α. This phenomenon can be understood as follows. The probability for the occurrence of a crisis is reduced for decreasing α due to the less pronounced eccentricity of the ellipse of fixed points, the reduced size of the local attractors of the destabilized modes, and the larger number of stable HGMs. Thus, for constant parameters except α, the shortened itinerancy and the reduced probability of a crisis substantially increase the chance that the trajectory reaches one of the stable HGMs. Consequently, the coexistence regions extend in γ-I space for decreasing α.

2. Increased stability of the stable state

As for all delay systems, a detailed linear stability analysis for semiconductor lasers subject to optical feedback is very difficult. Up to now, a linear stability analysis has only been performed for the maximum gain mode [24]. Detailed theoretical information about the stability properties of the other HGMs, which are particularly important in the context of the present paper, is still lacking. Even though the operation of semiconductor lasers on the stable HGMs has been observed in recent experiments for strong to moderate optical feedback [13] and for weak optical feedback [26], the stability of the HGMs has not yet been investigated experimentally. In our experiments, we address these stability properties of the HGMs for moderate to strong optical feedback and their dependence on α. We find that the time intervals of stable emission on one of the stable HGMs lengthen substantially with decreasing α; the stability of the stable emission state increases. Phenomenologically, this indicates that the activation energy [27] necessary to kick the trajectory off the stable HGMs increases for decreasing α. We point out that these interesting properties provide a new concept for the realization of a stable laser emission mode even for moderate to strong optical feedback. By reducing α, we directly control the nonlinearity and, thus, the stability properties of the system in order to achieve stable laser emission on one of the HGMs.

3. Coexistence of CC and stable emission

The scope of the presented experimental results also includes new aspects for the fundamental structure of the fully developed CC. For the lowest value of $\alpha=1.6(\pm 0.3)$, we observe coexistence of stable emission on a single high-gain external-cavity mode with fully developed CC dynamics.

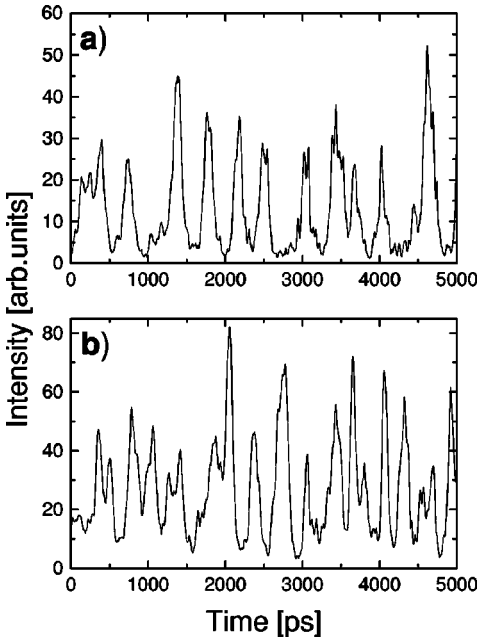

FIG. 6. Streak camera single-shot measurements of the intensity time series. (a) Low-frequency fluctuations regime; (b) fully developed coherence collapse regime. The parameters correspond to the time series depicted in Fig. 4 (top, middle).

This gives evidence that the stabilizing effects of a reduction of α can compensate for the destablizing effect of an increased injection current. Yet a sufficiently low value of α is required. If α is too large, stable emission does not occur within the CC regime although at least one stable mode should exist even under these conditions [25].

We note that for $\alpha=1.6(\pm 0.3)$, the signature of the stable state remains unchanged while the coexisting state undergoes a continuous transition from LFF to the fully developed CC. We have investigated this transition by single-shot streak camera measurements both for LFF and CC conditions. Figures 6(a) and 6(b) show intensity time series recorded within the LFF regime and the CC regime, respectively. The experimental conditions correspond to those of the oscilloscope time series shown in Fig. 4 (top, middle). Under both conditions, the system shows the characteristic fast pulsing dynamics. The pulse width as well as the average time interval between the pulses decrease for increasing injection current. The modulation depth of the pulses is slightly reduced in the CC regime. However, pronounced qualitative changes of the dynamical behavior of the system on a picosecond time scale do not occur.

The apparent differences between LFF and CC on slower time scales shown in Fig. 4 are caused by the following effects. First, increasing the injection current decreases the time intervals between the dropouts. Second, the probability of a crisis increases with increasing injection current. Thus, within the CC regime, a crisis can also occur on attractor ruins far away from maximum gain. Consequently, for sufficiently high injection currents, the drift of the trajectory towards high gain is usually interrupted much earlier, so that distinct dropouts cannot be identified any more. However, the fundamental mechanisms underlying to LFF and fully developed CC appear to be the same.

4. Properties of the LFF regime

The feedback induced instabilities causing the LFF are known to disappear below a critical value of α, typically for $\alpha \leqslant 1$ [11]. In our experiments, as can be seen from the drastic extension of the coexistence region and the very long duration of the stable emission states, we came close to this critical value, but could not finally reach it. Our experiments show that the instablility causing the LFF has not yet disappeared.

The slight shift of the feedback-reduced threshold and the LFF regime in γ-I space is due to the shift of the lasing wavelength along the gain curve away from the gain maximum. The gain of the laser decreases with decreasing wavelength, which results in an increase of the lasing threshold for a given amount of optical feedback. A more detailed investigation of the dependence of the average time intervals between two subsequent LFF intensity dropouts on α is a subject of future studies. In this context, we point out that the apparently stable emission between the intensity dropouts in the LFF state must not be confused with the stable emission on a single external-cavity mode which coexists with the LFF behavior for parameters corresponding to the coexistence regime.

V. CONCLUSIONS AND OUTLOOK

In conclusion, we have investigated the dynamical behavior of semiconductor lasers subject to delayed optical feedback in dependence on α accounting for the nonlinear amplitude-phase coupling of the optical field present in semiconductor lasers. We have controlled α by tuning the emission wavelength of the laser away from its solitary gain maximum using an intracavity etalon. We find that the value of α decreases continously with decreasing wavelengths, which is mainly due to the strong increase of the differential gain.

By recording detailed γ-I-space diagrams for several different values of α, we have identified and characterized the parameter ranges of the occurring dynamical regimes. In particular, we have demonstrated a very sensitive dependence of the dynamical behavior of the system on α: the regime of coexistence of LFF and stable emission on a single high-gain external-cavity mode enlarges drastically with decreasing α. Furthermore, the time intervals of stable emission prolong substantially. Thus, the stability of the stable emission state increases with decreasing α.

According to an analysis of the Lang-Kobayashi rate equation model, the relevant mechanism underlying the observed dynamical behavior can be understood as itinerancy towards the HGM followed either by a crisis or a jump of the trajectory on a stable fixed point. We have demonstrated that the structure of the fixed point solutions of the rate equations among which the trajectory itinerates is strongly dependent on α: a reduction of α reduces the probability for the occurrence of a crisis, and shortens the itinerancy of the trajectory towards one of the stable HGMs. Consequently, the parameter region of coexistence of LFF with stable emission enlarges, and the stability of the stable HGMs increases.

For the lowest value of α, we have observed even coexistence of fully developed CC with stable emission. Streak camera single shot measurements demonstrate similar fast pulsing dynamics of the laser operating in both the LFF regime and the CC regime. The signature of the coexisting stable state remains unchanged. These results indicate that the dynamical mechanism underlying LFF and CC is essentially the same.

Based on this detailed understanding of the dynamical behavior of semiconductor lasers subject to delayed optical feedback, future research may concentrate on the following two points. First, the experimental results presented in this paper demonstrate that the main nonlinearity of external cavity semiconductor lasers can be tailored for a single laser in a well controlled way without changing other experimental conditions. This variable nonlinearity of the system in combination with recent theoretical advances in the analysis and identification of delay systems [28,29] makes semiconductor laser subject to delayed optical feedback an even more attractive model system for further experimental investigations of fundamental phenomena of nonlinear dynamics. Second, our experiments have demonstrated that semiconductor lasers showing feedback-induced instabilities can be stabilized by a sufficient reduction of α: by appropriately shifting the emission wavelength of the laser away from its solitary gain maximum towards shorter wavelengths, α can be reduced below the critical value, so that the instabilities disappear. This new concept stabilizes the laser emission by directly controlling the nonlinearity and, consequently, the stability properties of the system. In general, semiconductor lasers with a sufficiently low α would be most interesting for practical applications due to the possibility of chirpless operation, and the insensitivity to delayed optical feedback. The design of such lasers requires a strong spectral dependence of the differential gain. Furthermore, for vanishing α, the maximum of the differential gain should be within the gain profile of the laser in order to allow a sufficiently large detuning of the emission wavelength. This seems to be possible in modulation-doped, strained quantum-well DFB lasers [30] in which the Bragg mirrors are appropriately detuned relative to the gain profile of the semiconductor material.

ACKNOWLEDGMENTS

The authors would like to thank C. R. Mirasso and G. H. M. van Tartwijk for helpful discussions. The authors acknowledge financial support from the Deutsche Forschungsgemeinschaft within the Sonderforschungsbereich 185.

[1] J. O'Gorman, B. J. Hawdon, P. Jenkins, J. Hegarty, and D. M. Heffernan, J. Mod. Opt. **38**, 1243 (1991).

[2] J. Ye, H. Li, and J. G. McInerny, Phys. Rev. A **47**, 2249 (1993).

[3] K. Ikeda and K. Matsumoto, Physica D **29**, 223 (1987).

[4] I. Fischer, O. Hess, W. Elsäßer, and E. O. Göbel, Phys. Rev. Lett. **73**, 2188 (1994).

[5] I. Fischer, G. H. M. van Tartwijk, A. M. Levine, W. Elsäßer, E. O. Göbel, and D. Lenstra, Phys. Rev. Lett. **76**, 220 (1996).

[6] H. Haug and H. Haken, Z. Phys. **204**, 262 (1967).

[7] C. H. Henry, IEEE J. Quantum Electron. **QE-18**, 259 (1982).
[8] G. P. Agrawal and N. K. Dutta, *Long Wavelength Semiconductor Lasers* (Van Nostrand Reinhold, New York, 1986).
[9] The overall gain profile of the system can be described as the superposition of the gain curve of the solitary laser, the Airy transmission function of the etalon, and the effective reflectivity of MO and feedback mirror.
[10] M. Hofmann, M. Koch, H. J. Heinrich, G. Weiser, J. Feldmann, W. Elsäßer, E. O. Göbel, W. W. Chow, and S. W. Koch, IEE Proc.-J: Optoelectron. **141**, 127 (1994).
[11] A. T. Ryan, G. P. Agrawal, G. R. Gray, and E. C. Gage, IEEE J. Quantum Electron. **QE-30**, 668 (1994).
[12] C. Masoller and N. B. Abraham, Phys. Rev. A **57**, 1313 (1998).
[13] T. Heil, I. Fischer, and W. Elsäßer, Phys. Rev. A **58**, R2672 (1998).
[14] R. Lang and K. Kobayashi, IEEE J. Quantum Electron. **QE-16**, 347 (1980).
[15] K. Vahala, L. C. Chiu, S. Margalit, and A. Yariv, Appl. Phys. Lett. **42**, 631 (1983).
[16] I. D. Henning and J. V. Collins, Electron. Lett. **19**, 927 (1983).
[17] B. W. Hakki and T. L. Paoli, J. Appl. Phys. **46**, 1299 (1975).
[18] M. Osinski and J. Buus, IEEE J. Quantum Electron. **QE-23**, 9 (1987).
[19] J. Mørk, B. Tromborg, and P. L. Christiansen, IEEE J. Quantum Electron. **QE-24**, 123 (1988).
[20] D. W. Sukow, J. R. Gardner, and D. J. Gauthier, Phys. Rev. A **56**, R3370 (1997).
[21] G. Huyet, S. Balle, M. Giudici, G. Giacomelli, and J. R. Tredicce, Opt. Commun. **149**, 341 (1998).
[22] T. Sano, Phys. Rev. A **50**, 2719 (1994).
[23] G. H. M. van Tartwijk, A. M. Levine, and D. Lenstra, IEEE J. Sel. Top. Quantum Electron. **1**, 466 (1995).
[24] A. M. Levine, G. H. M. van Tartwijk, D. Lenstra, and T. Erneux, Phys. Rev. A **52**, R3436 (1995).
[25] J. Wieland, C. R. Mirasso, and D. Lenstra, Opt. Lett. **22**, 469 (1997).
[26] A. Hohl and A. Gavrielides, Opt. Lett. **23**, 1606 (1998).
[27] R. Graham and T. Tél, Phys. Rev. A **33**, 1322 (1986).
[28] M. J. Bünner, T. Meyer, A. Kittel, and J. Parisi, Phys. Rev. E **56**, 5083 (1997).
[29] R. Hegger, M. J. Bünner, H. Kantz, and A. Giaquinta, Phys. Rev. Lett. **81**, 558 (1998).
[30] T. Yamanaka, Y. Yoshikuni, W. Lui, K. Yokoyama, and S. Seki, IEEE Photonics Technol. Lett. **4**, 1318 (1992).